

Itinerant ferromagnetism of two-dimensional repulsive fermions with Rabi coupling

V. Penna

Dipartimento di Fisica, Politecnico di Torino, and CNISM, Corso Duca degli Abruzzi 24, I-10129 Torino, Italy

L. Salasnich

Dipartimento di Fisica e Astronomia “Galileo Galilei” and CNISM, Università di Padova, Via Marzolo 8, I-35131 Padova, Italy
Istituto Nazionale di Ottica (INO) del Consiglio Nazionale delle Ricerche (CNR), Via Nello Carrara 1, I-50019 Sesto Fiorentino, Italy

Abstract. We study a two-dimensional fermionic cloud of repulsive alkali-metal atoms characterized by two hyperfine states which are Rabi coupled. Within a variational Hartree-Fock scheme, we calculate analytically the ground-state energy of the system. Then we determine the conditions under which there is a quantum phase transition with spontaneous symmetry breaking from a spin-balanced configuration to a spin-polarized one, an effect known as itinerant ferromagnetism. Interestingly, we find that the transition appears when the interaction energy per particle exceeds both the kinetic energy per particle and the Rabi coupling energy. The itinerant ferromagnetism of the polarized phase is analyzed, obtaining the population imbalance as a function of interaction strength, Rabi coupling, and number density. Finally, the inclusion of an external harmonic confinement is investigated by adopting the local density approximation. We predict that a single atomic cloud can display population imbalance near the center of the trap and a fully balanced configuration at the periphery.

1. Introduction

Recently, artificial spin-orbit and Rabi couplings have been implemented by means of counterpropagating laser beams in bosonic [1, 2] and fermionic [3, 4] atomic gases. These laser beams couple two internal hyperfine states of the atom by a stimulated two-photon Raman transition [1, 2, 3, 4]. Triggered by these remarkable experiments, in the last few years a large number of theoretical papers have analyzed the spin-orbit effects with Rashba [5] and Dresselhaus [6] terms in Bose-Einstein condensates [7, 8, 9, 10, 11, 12, 13] and also in the BCS-BEC crossover of superfluid fermions [14, 15, 16, 17, 18, 19, 20, 21, 22]. Very recently, the Rashba spin-orbit coupling in a two-dimensional (2D) repulsive Fermi gas has been investigated in [23, 24], where the density of states is quite simple and analytical results can be obtained. We stress that 2D quantum systems show peculiar physical properties and are crucial for technological applications: high-temperature superconductivity is attributed to materials characterized by a 2D-like transport [25], and, more generally, superconductor and oxide interfaces containing 2D electron gas are of paramount importance for contemporary electronics [26].

The Rabi coupling of hyperfine states of atoms is now a common tool for experimental and theoretical investigations involving multi-component gases. Some examples are: the control of the population of the hyperfine levels [27, 28], the formation of localized structures [29], and the mixing-demixing dynamics of Bose-Einstein condensates [30]. It is particularly interesting to study how the Rabi coupling affects the equilibrium properties of an atomic two-dimensional repulsive Fermi gas, and, more specifically, if the Rabi coupling can help a gas of spin-up and spin-down fermions to become ferromagnetic, thus determining the itinerant ferromagnetism proposed in [31]. The repulsive interaction induces the well-known Stoner instability [32] above a critical strength. Nevertheless, in the absence of the Rabi coupling this instability is expected to produce phase separation rather than spin flip [33]. Generally speaking, itinerant ferromagnetism is signaled by the spontaneous appearance of local spin imbalance, but this itself doesn't require spin flip mechanisms. A thorough investigation of this instability critical strength has been developed in [34, 35, 36, 37]. The observation of itinerant ferromagnetism in ultracold atoms in 3D is complicated by the presence of three-body losses [38], which are however expected to be less important in reduced dimensions [39]. As noted in Ref. [40], the itinerant ferromagnetism is a key effect to get a deeper insight in the physics of systems such as metals, quark liquids in neutron stars. Moreover, it is still debated whether homogeneous electron systems can reach a fully ferromagnetic state. We stress that very recently the observation of the ferromagnetic instability has been reported in a binary spin-mixture of ultracold ${}^6\text{Li}$ atoms [41].

In this paper we study a Rabi-coupled fermionic gas of repulsive alkali-metal atoms trapped in a quasi two-dimensional configuration, where the effects of the third direction are fully frozen due to a strong external confinement in that direction [42]. Itinerant ferromagnetism in a trapped repulsive 2D Fermi system, but without Rabi coupling,

has been investigated both analytically [43, 44] and numerically [45]. The fermionic atoms are characterized by two hyperfine internal states which can be modelled as two spin components. Here we investigate the ground-state properties of the quantum gas by using the Hartree-Fock method in the form of a mean-field approximation for operator products, where the population imbalance is a variational parameter. In this way we calculate analytically the conditions under which there is a quantum phase transition from a spin-balanced to a spin-polarized configuration. This phase transition features a spontaneous symmetry breaking of the fermion polarization (population imbalance) between two degenerate values. The behavior of the population imbalance is determined as a function of the system parameters. We also consider the inclusion of an external harmonic potential investigating non-trivial effects caused by the space-dependent confinement on the polarization of the atomic cloud.

2. Model Hamiltonian

The many-body Hamiltonian of the 2D fermionic atomic gas including contact interactions of strength g and Rabi coupling of frequency Ω reads

$$\hat{H} = \int d^2\mathbf{r} \left[\sum_{\sigma=\uparrow,\downarrow} \hat{\psi}_\sigma^\dagger \left(-\frac{\hbar^2}{2m} \nabla^2 \right) \hat{\psi}_\sigma + g \hat{\psi}_\uparrow^\dagger \hat{\psi}_\downarrow^\dagger \hat{\psi}_\downarrow \hat{\psi}_\uparrow + \frac{\hbar\Omega}{2} \left(\hat{\psi}_\uparrow^\dagger \hat{\psi}_\downarrow + \hat{\psi}_\downarrow^\dagger \hat{\psi}_\uparrow \right) \right], \quad (1)$$

where $\hat{\psi}_\sigma(\mathbf{r})$ is the field operator which destroys a fermion of spin σ at position \mathbf{r} . It is important to stress that, due to the presence of the Rabi coupling, the total number

$$\hat{N} = \int d^2\mathbf{r} \left(\hat{\psi}_\uparrow^\dagger(\mathbf{r}) \hat{\psi}_\uparrow(\mathbf{r}) + \hat{\psi}_\downarrow^\dagger(\mathbf{r}) \hat{\psi}_\downarrow(\mathbf{r}) \right), \quad (2)$$

is a constant of motion, while the relative numbers \hat{N}_\uparrow and \hat{N}_\downarrow are not.

Applying the mean-field approximation for operator products (see, e.g., [46], [47]) to

$$\hat{\psi}_\uparrow^\dagger \hat{\psi}_\downarrow^\dagger \hat{\psi}_\downarrow \hat{\psi}_\uparrow \simeq n_\downarrow \hat{\psi}_\uparrow^\dagger \hat{\psi}_\uparrow + n_\uparrow \hat{\psi}_\downarrow^\dagger \hat{\psi}_\downarrow - n_\uparrow n_\downarrow, \quad (3)$$

with $n_\sigma = \langle \hat{n}_\sigma \rangle = \langle \hat{\psi}_\sigma^\dagger \hat{\psi}_\sigma \rangle$ ($\sigma = \uparrow, \downarrow$), enables us to write the mean-field many-body Hamiltonian as

$$\hat{H} = \int d^2\mathbf{r} \left[\left(\hat{\psi}_\uparrow^\dagger, \hat{\psi}_\downarrow^\dagger \right) \mathcal{H} \begin{pmatrix} \hat{\psi}_\uparrow \\ \hat{\psi}_\downarrow \end{pmatrix} \right] - \frac{gn^2}{4} (1 - \zeta^2) L^2, \quad (4)$$

where L^2 is the area of the 2D system and \mathcal{H} is the single-particle matrix Hamiltonian

$$\mathcal{H} = \begin{pmatrix} -\frac{\hbar^2}{2m} \nabla^2 + \frac{gn}{2} (1 + \zeta) & \frac{\hbar\Omega}{2} \\ \frac{\hbar\Omega}{2} & -\frac{\hbar^2}{2m} \nabla^2 + \frac{gn}{2} (1 - \zeta) \end{pmatrix} \quad (5)$$

with the average total number density and the population imbalance given by

$$n = n_\uparrow + n_\downarrow, \quad \zeta = \frac{n_\downarrow - n_\uparrow}{n}, \quad (6)$$

respectively. Clearly, at fixed total density n , one finds that $\zeta \in [-1, 1]$. It is important to stress that, within our Hartree-Fock scheme, ζ is a variational parameter which must be determined by minimizing the energy of the system. By using the Pauli matrices σ_z and σ_x such that $[\sigma_a, \sigma_b] = i\epsilon_{abc}\sigma_c$, with indexes $a, b, c = x, y, z$, the single-particle Hamiltonian (5) takes the form

$$\mathcal{H} = \left(-\frac{\hbar^2}{2m} \nabla^2 + \frac{gn}{2} \right) \mathcal{I} + \frac{gn}{2} \zeta \sigma_z + \frac{\hbar\Omega}{2} \sigma_x .$$

The latter can be diagonalized exactly [48], and one finds

$$\mathcal{H}|\mathbf{k}, s\rangle = E_{\mathbf{k},s}|\mathbf{k}, s\rangle , \quad (7)$$

where the eigenvalue

$$E_{\mathbf{k},s} = \frac{\hbar^2 k^2}{2m} + \alpha_s \quad (8)$$

depends on the two-dimensional wavevector \mathbf{k} , the index $s = -1, +1$ is the eigenvalue of σ_z , and

$$\alpha_s = \frac{g}{2}n + \frac{s}{2} \sqrt{g^2 n^2 \zeta^2 + \hbar^2 \Omega^2} \quad (9)$$

is the contribution to the single-particle energy due to the repulsive interaction of strength g ($g > 0$) and the Rabi coupling of frequency Ω . The corresponding eigenstates are given by

$$|\mathbf{k}, s\rangle = \frac{e^{i\mathbf{k}\cdot\mathbf{r}}}{L} S|s\rangle,$$

where $\sigma_z|s\rangle = s|s\rangle$, $\vec{p}|\mathbf{k}, s\rangle = \hbar\mathbf{k}|\mathbf{k}, s\rangle$ and $S = \exp(i\phi\sigma_y/2)$, with $\text{tg}\phi = \hbar\Omega/gn$, is the transformation taking \mathcal{H} into the diagonal form. It follows that the mean-field many-body Hamiltonian can be written as

$$\hat{H} = -\frac{gn^2}{4}(1 - \zeta^2)L^2 + \sum_{\mathbf{k}} \sum_{s=-1,1} E_{\mathbf{k},s} \hat{b}_{\mathbf{k},s}^+ \hat{b}_{\mathbf{k},s}, \quad (10)$$

where $\hat{b}_{\mathbf{k},s}$ and $\hat{b}_{\mathbf{k},s}^+$ are ladder operators which destroy and create a fermion in the single-particle state $|\mathbf{k}, s\rangle$.

3. Ground-state properties

By implementing the continuum limit $\sum_{\mathbf{k}} \rightarrow L^2 \int d^2\mathbf{k}/(2\pi)^2$, the average total number density $n = N/L^2$ of the fermionic system is found to be

$$n = \sum_{s=-1,1} \int \frac{d^2\mathbf{k}}{(2\pi)^2} \langle \hat{b}_{\mathbf{k},s}^+ \hat{b}_{\mathbf{k},s} \rangle, \quad (11)$$

while the average internal-energy density $\mathcal{E} = E/L^2$ reads

$$\mathcal{E} = -\frac{gn^2}{4}(1 - \zeta^2) + \sum_{s=-1,1} \int \frac{d^2\mathbf{k}}{(2\pi)^2} E_{\mathbf{k},s} \langle \hat{b}_{\mathbf{k},s}^+ \hat{b}_{\mathbf{k},s} \rangle. \quad (12)$$

Moreover, at zero temperature one can write

$$\langle \hat{b}_{\mathbf{k},s}^+ \hat{b}_{\mathbf{k},s} \rangle = \Theta(\mu - E_{\mathbf{k},s}), \quad (13)$$

where $\Theta(x)$ is the Heaviside step function and μ is the zero-temperature chemical potential, namely, the Fermi energy of the interacting system. Notice that μ is fixed by the conservation of the total number of fermions. Then, by using Eq. (13), from Eqs. (11) and (12) we find

$$n = \frac{1}{4\pi} \left(\frac{2m}{\hbar^2} \right) [(\mu - \alpha_{-1}) \Theta(\mu - \alpha_{-1}) + (\mu - \alpha_{+1}) \Theta(\mu - \alpha_{+1})] \quad (14)$$

and

$$\begin{aligned} \mathcal{E} = & -\frac{gn^2}{4}(1 - \zeta^2) + \frac{1}{8\pi} \left(\frac{2m}{\hbar^2} \right) [(\mu^2 - \alpha_{-1}^2) \Theta(\mu - \alpha_{-1}) \\ & + (\mu^2 - \alpha_{+1}^2) \Theta(\mu - \alpha_{+1})]. \end{aligned} \quad (15)$$

Clearly, if $\mu \leq \alpha_-$ there are no solutions. Let us now consider the remaining cases $\mu < \alpha_+$ and $\alpha_+ \leq \mu$.

Regime $\mu < \alpha_+$

From Eqs. (9), (14) and (15), under the condition $\mu < \alpha_{+1}$, we obtain

$$\mu = \frac{4\pi\hbar^2}{2m} n + \frac{1}{2}gn - \frac{1}{2}\sqrt{g^2n^2\zeta^2 + \hbar^2\Omega^2} \quad (16)$$

and also

$$\mathcal{E} = -\frac{gn^2}{4}(1 - \zeta^2) + \frac{n}{2} \left[\left(g + \frac{4\pi\hbar^2}{2m} \right) n - \sqrt{g^2n^2\zeta^2 + \hbar^2\Omega^2} \right], \quad (17)$$

where Eq. (16) has been used to express \mathcal{E} in terms of n instead of μ . This average energy density \mathcal{E} is a function of the population imbalance ζ , which is our variational parameter. For the sake of simplicity we introduce the characteristic energies

$$E_\Omega = \hbar\Omega, \quad E_{int} = gn, \quad E_{kin} = \frac{4\pi\hbar^2n}{2m}.$$

The minimum of \mathcal{E} with respect to ζ is easily found from the condition $\partial\mathcal{E}/\partial\zeta = 0$ which, written in terms of E_{int} and E_Ω , gives

$$\frac{n}{2}E_{int}\zeta \left(1 - \frac{E_{int}}{\sqrt{E_{int}^2\zeta^2 + E_\Omega^2}} \right) = 0. \quad (18)$$

Consequently, one has two cases: $\zeta = 0$ for $E_{int} \leq E_\Omega$, and $\zeta = \pm\sqrt{1 - E_\Omega^2/E_{int}^2}$ for $E_\Omega < E_{int}$. In the second case, the solution $\zeta = 0$ describes a maximum separating the two minima. This scenario is completed by taking into account the condition $\mu < \alpha_+$ characterizing the present regime, with μ given by Eq. (16), finding

$$E_{kin} < \sqrt{E_{int}^2\zeta^2 + E_\Omega^2}. \quad (19)$$

Then, the two cases described above can be detailed as follows.

Condition A: For $E_{int} \leq E_\Omega$ and $E_{kin} < E_\Omega$ the population imbalance is

$$\zeta_A = 0, \quad (20)$$

and the corresponding chemical potential and energy density are given by

$$\mu_A = \frac{1}{2}E_{int} + E_{kin} - \frac{1}{2}E_\Omega, \quad \mathcal{E}_A = \frac{n}{4}E_{int} + \frac{n}{2}(E_{kin} - E_\Omega). \quad (21)$$

Condition B: For $E_\Omega < E_{int}$ and $E_{kin} < E_{int}$ the population imbalance is

$$\zeta_B = \pm \sqrt{1 - \left(\frac{E_\Omega}{E_{int}}\right)^2}, \quad (22)$$

which shows the double degeneracy of the ground state and entails a spontaneous symmetry breaking, while

$$\mu_B = E_{kin}, \quad \mathcal{E}_B = \frac{n}{2} \left(E_{kin} - \frac{E_\Omega^2}{2E_{int}} \right) \quad (23)$$

represent the chemical potential and energy density, respectively. The results under the condition B) show explicitly that there is population imbalance if the interaction energy per particle E_{int} is larger than both the kinetic term E_{kin} (proportional to the kinetic energy per particle $\pi\hbar^2 n/(2m)$) and the Rabi energy E_Ω . This is a clear example of Stoner instability [32], where a sufficiently large repulsion between fermions makes the uniform and balanced system unstable. In this case, due to the presence of Rabi coupling, the system becomes polarized being either $n_\uparrow > n_\downarrow$ ($\zeta_B < 0$) or $n_\uparrow < n_\downarrow$ ($\zeta_B > 0$).

Regime $\alpha_+ \leq \mu$

From Eqs. (9), (14) and (15), under the condition $\alpha_{+1} \leq \mu$, we obtain

$$\mu = \frac{1}{2}(E_{kin} + E_{int}) \quad (24)$$

and the ground-state energy

$$\mathcal{E} = \frac{n}{4} \left[E_{int} \zeta^2 \left(1 - \frac{E_{int}}{E_\Omega} \right) + 2E_{int} + E_{kin} - \frac{E_\Omega^2}{E_{kin}} \right] \quad (25)$$

by using Eq. (24) to express \mathcal{E} in terms of n instead of μ . Also in this case the average energy density \mathcal{E} is a function of the population imbalance ζ , which is our variational parameter. However, the functional dependence of (25) on ζ is quite different with respect to (17).

Finding the minimum of \mathcal{E} , given by Eq. (25), with respect to ζ gives two cases: $\zeta = 0$ for $E_{int} < E_{kin}$, and $\zeta = \pm 1$ for $E_{kin} < E_{int}$. Again, one must include the condition $\alpha_+ \leq \mu$, with μ given by Eq. (24), obtaining

$$\sqrt{\zeta^2 E_{int}^2 + E_\Omega^2} \leq E_{kin}. \quad (26)$$

One easily discovers that the second case described above ($\zeta = \pm 1$ for $E_{kin} < E_{int}$) is incompatible with (26) and it must be excluded. By taking into account (26), the remaining case characterized by $E_{int} < E_{kin}$ can be detailed as follows.

Condition C: For $E_{int} \leq E_{kin}$ and $E_{\Omega} \leq E_{kin}$ the population imbalance

$$\zeta_C = 0, \quad (27)$$

entails

$$\mu_C = \frac{1}{2}(E_{int} + E_{kin}), \quad \mathcal{E}_C = \frac{n}{4} \left(E_{int} + E_{kin} - \frac{E_{\Omega}^2}{E_{kin}} \right) \quad (28)$$

representing the chemical potential and energy density, respectively, of this case.

The analysis so far developed clearly shows that only under the condition B) there is itinerant ferromagnetism in the two-dimensional repulsive Fermi gas. The condition B) means that the interaction energy per particle E_{int} must be larger than both the kinetic energy per particle E_{kin} and the Rabi energy E_{Ω} . To summarize, this result is convenient to introduce the Fermi energy ϵ_F of our 2D fermionic system in the absence of interaction and Rabi coupling, that is given by

$$\epsilon_F = \frac{\hbar^2}{m} \pi n. \quad (29)$$

Taking into account the conditions A, B, C described in the previous Section, the chemical potential of the system in the presence of interaction and Rabi coupling can be then written as

$$\mu = \begin{cases} \epsilon_F + \frac{1}{2}E_{int} & \text{for } E_{int} \leq 2\epsilon_F \\ 2\epsilon_F & \text{for } E_{int} > 2\epsilon_F \end{cases} \quad (30)$$

under the condition $E_{\Omega} \leq 2\epsilon_F$, and

$$\mu = \begin{cases} 2\epsilon_F - \frac{1}{2}(E_{\Omega} - E_{int}) & \text{for } E_{int} \leq E_{\Omega} \\ 2\epsilon_F & \text{for } E_{int} > E_{\Omega} \end{cases} \quad (31)$$

under the condition $E_{\Omega} > 2\epsilon_F$. In the upper panel of Fig. 1 we report the adimensional chemical potential μ/ϵ_F as a function of the adimensional interaction strength $E_{int}/(2\epsilon_F)$ for two values of adimensional Rabi energy $E_{\Omega}/(2\epsilon_F)$. The figure clearly shows that at the critical strength there is the derivative of the chemical potential changes slope.

The region where $\mu = 2\epsilon_F$ corresponds to the condition B: the system becomes spin-polarized. In the lower panel of Fig. 1 we plot the population imbalance $|\zeta|$ as a function of the adimensional interaction strength $gn/(2\epsilon_F)$ for two values of adimensional Rabi energy $E_{\Omega}/(2\epsilon_F)$. As shown in the figure, the population imbalance ζ , given by Eq. (22), decreases by increasing the Rabi frequency Ω . This result is consistent with previous two-dimensional calculations [34, 35, 36, 37] which suggest, in the absence of Rabi coupling, a jump from $\zeta = 0$ to $\zeta = \pm 1$ at the critical strength $g_c = 4\pi\hbar^2/(2m) = E_{kin}/n$. Notice that this jump can be softened also by beyond-mean-field quantum effects [34] or spin-orbit couplings [36]. Our results on the order parameter ζ , and specifically the lower panel of Fig. 1, signal a first-order phase transition if $E_{\Omega}/(2\epsilon_F) < 1$ and a second-order phase transition if $E_{\Omega}/(2\epsilon_F) > 1$.

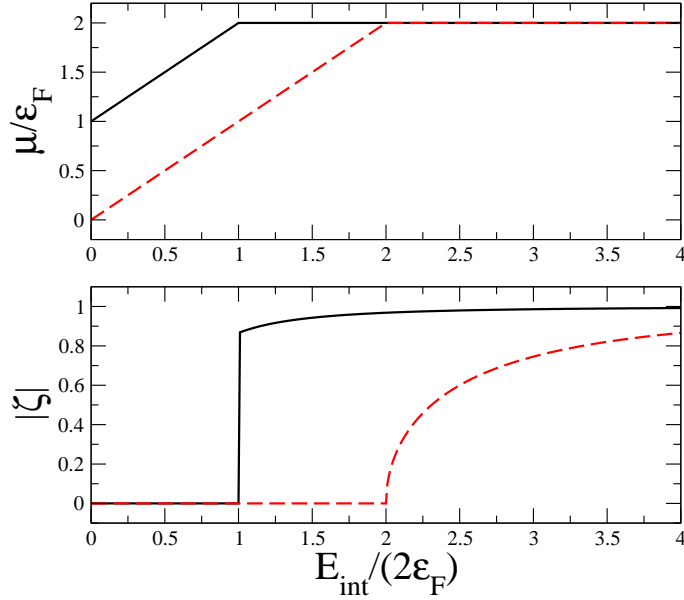


Figure 1. Upper panel: adimensional chemical potential μ/ϵ_F as a function of the adimensional interaction strength $E_{int}/(2\epsilon_F)$ for two values of adimensional Rabi energy $E_\Omega/(2\epsilon_F)$: 1/2 (solid line) and 2 (dashed line). Lower panel: absolute value $|\zeta|$ of the population imbalance as a function of the adimensional interaction strength $E_{int}/(2\epsilon_F)$ for the same two values of adimensional Rabi energy $E_\Omega/(2\epsilon_F)$.

4. Discussion and inclusion of harmonic confinement

Up to now we have considered a 2D homogeneous fermionic system. Here we discuss the effect of an external harmonic confinement

$$U(\mathbf{r}) = \frac{1}{2}m\omega^2(x^2 + y^2) \quad (32)$$

on the properties of the 2D system. We adopt the local density approximation [49]:

$$\bar{\mu} = \mu[n(\mathbf{r})] + U(\mathbf{r}), \quad (33)$$

where $\bar{\mu}$ is the chemical potential of the non uniform 2D system, $n(\mathbf{r}) = n_\uparrow(\mathbf{r}) + n_\downarrow(\mathbf{r})$ is the local number density with

$$N = \int d^2\mathbf{r} n(\mathbf{r}) \quad (34)$$

the total number of fermions, and $\mu[n]$ is the local chemical potential given by Eqs. (30) and (31). By using $r = \sqrt{x^2 + y^2}$ Eq. (33) can be written as

$$r = \frac{1}{\omega} \sqrt{2(\bar{\mu} - \mu[n])} \quad (35)$$

which gives the radial coordinate r as a function of the number density n . This formula can be easily implemented numerically to determine the density profile $n(r)$, the local population imbalance

$$\zeta(r) = \begin{cases} 0 & \text{for } n(r) \leq \frac{E_\Omega}{g} \\ \sqrt{1 - E_\Omega^2/(g^2 n^2(r))} & \text{for } n(r) > \frac{E_\Omega}{g} \end{cases}, \quad (36)$$

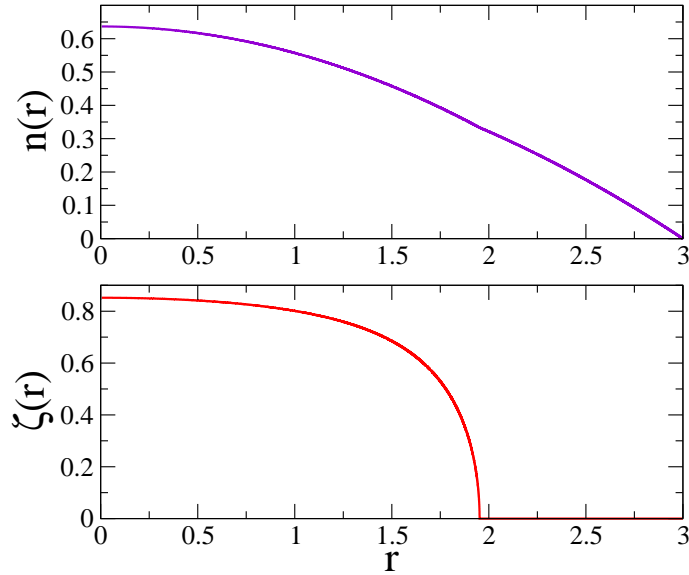


Figure 2. Total density profile $n(r)$ and population imbalance profile $\zeta(r)$ of the 2D Fermi gas under harmonic confinement of frequency ω . We set $\hbar = m = \omega = 1$ and choose $\Omega = 1$, $g = 3$, and $\bar{\mu} = 4$. The lower panel shows spin-flip (population imbalance) near the center of the trap while the periphery remains balanced.

and the local densities of fermions with spin up and spin down:

$$n_{\downarrow}(r) = \frac{1}{2}n(r)(1 + \zeta(r)) , \quad n_{\uparrow}(r) = \frac{1}{2}n(r)(1 - \zeta(r)) . \quad (37)$$

As an example, in Fig. 2 we report the total number density profile $n(r)$ (upper panel) and the population imbalance profile $\zeta(r)$ (lower panel) with a simple choice of the parameters which ensures that $n(0) > E_{\Omega}/g$. This condition is crucial to produce an atomic cloud with population imbalance. Note that the appearance of a non-zero population imbalance implies a spontaneous symmetry breaking of the ground-state with respect to the choice ζ or $-\zeta$.

In Fig. 3 we plot the corresponding local densities $n_{\downarrow}(r)$ and $n_{\uparrow}(r)$. The figures clearly show that the atomic cloud is characterized by population imbalance near the center of the trap ($r = 0$) where the total number density is larger than E_{Ω}/g . Instead, at the periphery (near the surface) of the atomic cloud the gas is fully balanced. We emphasize that setting $\hbar = m = \omega = 1$ (as done in Fig. 2 and Fig. 3) amounts to using harmonic-trap units: energies in units of $\hbar\omega$ and lengths in units of $a_H = \sqrt{\hbar/(m\omega)}$, that is the characteristic length of harmonic confinement.

In the experiments with ultracold atomic clouds having a quasi-2D disk-shaped configuration on the (x, y) plane, one finds typically $a_H \simeq 100 \mu\text{m}$, while the 2D interaction strength g reads $g = 4(\hbar\omega)a_s a_H^2/a_z$ with a_s the 3D s-wave scattering length and a_z the characteristic length of the confinement along the z axis. Remarkably, in current experiments the 3D s-wave scattering length a_s can be modified by using an external magnetic field (Fano-Feshbach resonance technique) and consequently one can easily move the system from a weakly-interacting to a strongly-interacting regime.

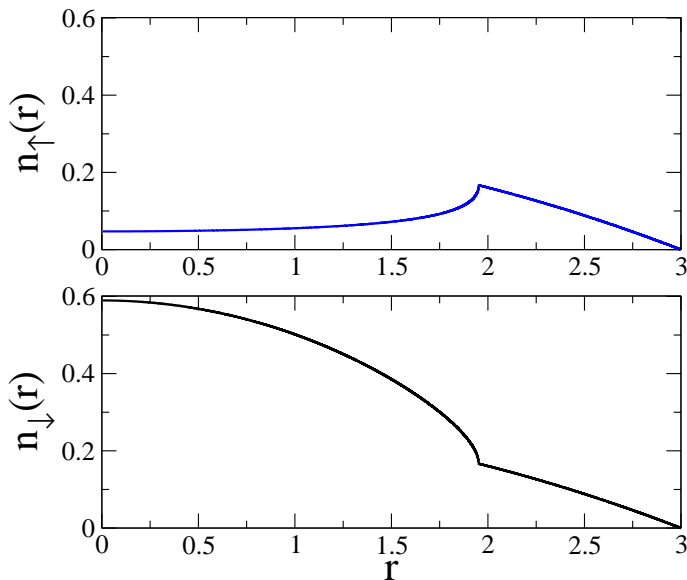


Figure 3. Local densities $n_{\downarrow}(r)$ and $n_{\uparrow}(r)$ of the 2D Fermi gas under harmonic confinement of frequency ω . We set $\hbar = m = \omega = 1$ and choose $\Omega = 1$, $g = 3$, and $\bar{\mu} = 4$. The panels clearly show the enhancement of the number of atoms with spin down near the center of the trap, while near the surface the system remains balanced.

5. Conclusions

In this paper we have shown how the non-trivial interplay among Pauli exclusion principle, repulsive interaction, and Rabi coupling can induce itinerant ferromagnetism in two-dimensional repulsive Fermi gases. In particular, we have analytically found that for a homogeneous 2D fermionic system there is polarization (i.e., itinerant ferromagnetism) when the interaction energy per particle is larger than both the kinetic energy per particle and the Rabi energy. It is important to stress that the itinerant ferromagnetism is certainly driven by the Stoner instability [32]: a sufficiently large repulsion between fermions make the uniform and balanced system unstable. However, as we have shown in this paper, it is the presence of Rabi coupling that allows the phenomenon of spin flip. In fact, in the absence of Rabi coupling or other spin-dependent mechanisms, the Stoner instability implies phase separation and not spin flip. Similar effects are expected in bosonic mixtures [30, 50]. Here we have adopted a Hartree-Fock mean-field approach. On the basis of previous results obtained in the absence of Rabi coupling in 2D and 3D [43, 45, 51], we expect that beyond-mean-field quantum fluctuations can slightly reduce the critical strength of Stoner instability.

In the last part of the paper we have considered the inclusion of an external harmonic potential, which is the simplest trapping configuration for experiments with ultracold alkali-metal atoms. In this case, we have predicted a remarkable effect we expect to be accessible in the near-future experiments: for a sufficiently large number of fermions, such that the number density at the center of the trap exceeds a critical value, the 2D fermionic gas is characterized by population imbalance near the center of

the trap and by a fully balanced configuration near the surface.

Acknowledgements

The authors thank Prof. Flavio Toigo for enlightening discussions and suggestions. LS acknowledges for partial support the 2016 BIRD project "Superfluid properties of Fermi gases in optical potentials" of the University of Padova.

References

- [1] Lin Y J, Jimenez-Garcia K, and Spielman I B 2011 *Nature* **471** 83
- [2] Zhang J-Y, Ji S-C, Chen Z, Zhang L, Du Z-D, Yan B, Pan G-S, Zhao B, Deng Y-J, Zhai H, Chen S, and Pan J W 2012 *Phys. Rev. Lett.* **109** 115301
- [3] Wang P, Yu Z-Q, Fu Z, Miao J, Huang L, Chai S, Zhai H, and Zhang J 2012 *Phys. Rev. Lett.* **109** 095301
- [4] Cheuk L W, Sommer A T, Hadzibabic Z, Yefsah T, Bakr W S, and Zwierlein M W 2012 *Phys. Rev. Lett.* **109** 095302
- [5] Bychkov Y A and Rashba E I 1984 *J. Phys. C* **17** 6029
- [6] Dresselhaus G 1955 *Phys. Rev.* **100** 580
- [7] Li Y, Pitaevskii L P, and Stringari S 2012 *Phys. Rev. Lett.* **108** 225301
- [8] Martone G I, Li Yun, Pitaevskii L P, and Stringari S 2012 *Phys. Rev. A* **86** 063621
- [9] Burrello M and Trombettoni A 2011 *Phys. Rev. A* **84** 043625
- [10] Merkl M, Jacob A, Zimmer F E, Ohberg P, and Santos L 2010 *Phys. Rev. Lett.* **104** 073603; Fialko O, Brand J, and Zulicke U 2012 *Phys. Rev. A* **85** 051605; Liao R, Huang Z-G, Lin X-M, and Liu W-M 2013 *ibid.* **87** 043605
- [11] Achilleos V, Frantzeskakis D J, Kevrekidis P G, and Pelinovsky D E 2013 *Phys. Rev. Lett.* **110** 264101
- [12] Xu Y, Zhang Y, and Wu B 2013 *Phys. Rev. A* **87** 013614
- [13] Salasnich L and Malomed B A 2013 *Phys. Rev. A* **87** 063625
- [14] Vyasanakere J P and Shenoy V B 2011 *Phys. Rev. B* **83** 094515; Vyasanakere J P, Zhang S, and Shenoy V B 2011 *Phys. Rev. B* **84** 014512
- [15] Gong M, Tewari S, and Zhang C 2011 *Phys. Rev. Lett.* **107** 195303
- [16] Hu H, Jiang L, Liu X-J, and Pu H 2011 *Phys. Rev. Lett.* **107** 195304
- [17] Iskin M and Subasi A L 2011 *Phys. Rev. Lett.* **107** 050402
- [18] Dell'Anna L, Mazzarella G, and Salasnich L 2011 *Phys. Rev. A* **84** 033633; Dell'Anna L, Mazzarella G, and Salasnich L 2012 *Phys. Rev. A* **86** 053632
- [19] Han Li and Sa de Melo C A R 2012 *Phys. Rev. A* **85** 011606(R)
- [20] Chen G, Gong M, and Zhang C 2012 *Phys. Rev. A* **85** 013601
- [21] Zhou K, Zhang Z 2012 *Phys. Rev. Lett.* **108** 025301
- [22] Yang X, Wan S 2012 *Phys. Rev. A* **85** 023633
- [23] Salasnich L 2013 *Phys. Rev. A* **88** 055601
- [24] Gigli L and Toigo F 2015 *J. Phys. B: At. Mol. Opt. Phys.* **48** 245302
- [25] Loktev V M, Quick R M, and Sharapov S G 2001 *Phys. Rep.* **349** 1
- [26] Ando T, Fowler A B, and Stern F 1982 *Rev. Mod. Phys.* **54** 437; Mannhart J, Blank D H A, Hwang H Y, Millis A J, and Triscone J-M 2008 *MRS Bull.* **33** 1027
- [27] Lewenstein M, Sanpera A, and Ahufinger V 2012 *Ultracold atoms in optical lattices: simulating quantum many-body systems* (Oxford: Oxford University Press).
- [28] Steck D A, *Quantum and Atom Optics*, available online at <http://steck.us/teaching>.
- [29] Horstmann B, Durr S, and Roscilde T 2010 *Phys. Rev. Lett.* **105** 160402

- [30] Nicklas E, Strobel H, Zibold T, Gross C, Malomed B A, Kevrekidis P G, and Oberthaler M K 2011 *Phys. Rev. Lett.* **107**, 193001
- [31] Jo G-B, Lee Y-R, Choi J-H, Christensen C A, Kim T H, Thywissen J H, Pritchard D E, and Ketterle W 2009 *Science* **325** 1521152
- [32] Stoner E C 1947 *Rep. Prog. Phys.* **11** 43
- [33] Salasnich L, Pozzi B, Parola A, and Reatto L 2000 *J. Phys. B* **33** 3943
- [34] Conduit G J, Green A G, and Simons B D 2009 *Phys. Rev. Lett.* **103** 207201
- [35] Massignan P, Yu Z, and Bruun G M 2013 *Phys. Rev. Lett.* **110**, 230401 (2013).
- [36] Ambrosetti A, Lombardi G, Salasnich L, Silvestrelli P L, and Toigo F 2014 *Phys. Rev. A* **90** 043614
- [37] Jiang Y, Kurlov D V, Guan Xi-W, Schreck F, Shlyapnikov G V 2016 *Phys. Rev. A* **94**, 011601(R) (2016).
- [38] Sanner C, Su E J, Huang W, Keshner A, Gillen J, and Ketterle W 2012 *Phys. Rev. Lett.* **108** 240404
- [39] Petrov D S and Shlyapnikov G V, 2001 *Phys. Rev. A* **64** 012706
- [40] Massignan P, Zaccanti M and Bruun G M 2014 *Rep. Prog. Phys.* **77** 034401
- [41] Valtolina G, Scazza F, Amico A, Burchianti A, Recati A, Enss T, Inguscio M, Zaccanti M, and Roati G 2016 arXiv:1605.07850
- [42] Salasnich L and Toigo F 2008 *J. Low Temp. Phys.* **150** 643; Mazzarella G, Salasnich L and Toigo F 2009 *Phys. Rev. A* **79** 023615
- [43] Conduit G J 2010 *Phys. Rev. A* **82** 043604
- [44] He L Y and Huang X G 2012 *Phys. Rev. A* **85** 043624
- [45] Conduit G J 2013 *Phys. Rev. B* **87** 184414
- [46] van Oosten D, van der Straten P, and Stoof H T C 2001 *Phys. Rev. A* **63** 053601
- [47] Buonsante P, Penna V, and Vezzani A 2005 *Laser Phys.* **15** 361
- [48] Penna V and Raffa F A 2014 *J. Phys. B: At. Mol. Opt. Phys.* **47** 075501
- [49] Lipparini E 2008 *Modern many-particle physics* (Singapore: World Scientific)
- [50] Lingua F, Guglielmino M, Penna V, and Capogrosso-Sansone B 2015 *Phys. Rev. A* **92** 053610
- [51] Pilati S, Bertaina G, Giorgini S, and Troyer M 2010 *Phys. Rev. Lett.* **105** 030405